Etching the Oxide Barrier of Micrometer-Scale Self-Organized Porous Anodic Alumina Membranes

Etching the Oxide Barrier of Micrometer-Scale Self-Organized Porous Anodic Alumina Membranes

Jonathan Bellemare,[z] Louis-Philippe Carignan, Frédéric Sirois, and David Ménard

Department of Engineering Physics, Polytechnique Montréal, Station Centre-ville, QC H3C 3A7, Canada

We develop a quantitative model to calculate the optimal experimental conditions for the etching of the oxide barrier of porous anodic alumina (PAA) membranes. The method is applied to a membrane fabricated at 370 V in a solution of 2% citric acid. The process creates a network of small pores at the bottom of the larger pores, which accelerates the oxide barrier etching relatively to the pore walls of the PAA membranes, when etched in a solution of phosphoric acid. The oxide barrier etching is confirmed by observation of PAA membranes using scanning electron microscopy, revealing the formation of the small pores and the preferential etching of the bottom of the pores rather than the pore walls. The proposed method, which leads to a better control over the fabrication of nanoporous templates, can be adapted to oxide barriers of different PAA membranes formed at different voltages and in different acids.

 [DOI: 10.1149/2.0791504jes]

Manuscript submitted October 13, 2014; revised manuscript received January 28, 2015. Published February 6, 2015.

Porous anodic alumina (PAA) membranes provide useful templates for fabricating nanostructures, such as nanowires,[1] nanotubules,[2] nanorods,[3] nanotubes,[4] and nanodots,[5] which can be exploited in technological applications. Current applications include, among others, human blood filters,[6] micrometer and nanometer filters,[7] and solar cells.[8] The PAA membranes, which are fabricated by electrochemical processes, exhibit a hexagonal array of vertical pores that are open on their surface and closed by an oxide barrier at the bottom. In order to obtain PAA membranes that are open on both sides, such as required in filter applications or when electrodepositing nanowires, one needs to develop a strategy for removing the oxide on the bottom side.

Several articles proposed methods to etch the oxide barrier of PAA membranes, each with their advantages and disadvantages. Han et al.[9] reported a straightforward method to etch the oxide barrier by first removing the PAA membranes from the growth foil, then by covering the open side with a protective polymer made of nitrocellulose and polyester resin, and finally by etching the membrane in phosphoric acid, 5 wt% at 30°C, until the dissolution of the oxide barrier. While this method is relatively simple and applicable to membranes grown at any voltage, that is, with various geometrical parameters, it requires the application of a protective polymer and its subsequent removal, a delicate operation since the membrane is quite fragile. Also, the polymer can contaminate the membrane. This method has been used in our group to fabricate arrays of ferromagnetic nanowires.[10]

Nielsch et al.[11] exploited the natural chemical widening of the pores of PAA membranes in order to decrease the voltage required for anodization due to the oxide barrier being thinner and allowing the formation of smaller pores in the oxide barrier. Their application of a constant current of 0.29 A/cm^2 during 15 min., followed by a constant current of 0.135 A/cm^2 also during 15 minutes, yielded a network of small open pores at the bottom surface. With this interesting in-situ method, the oxide layer is not always completely removed, but rather pierced, and it is also difficult to obtain the desired pore size, due to the initial chemical widening. This method was also used with membranes fabricated at 40 V, but no indication about how to extend it to other anodization voltages is provided in the paper.

Another approach used by Zhao et al.[12] is to etch the oxide barrier using a slowly decreasing voltage ramp, from 40 V to 15 V at a rate of 1 V per 9 s, in order to create a network of small pores at the bottom of the large pores in the PAA membrane, initially grown at 40 V. In this method, the membrane is initially dipped into a 0.5 M KCl solution and act as the cathode, whereas a graphite plate is used as the anode. Setting the potential difference at the PAA membrane and the graphite plate between −4 V and −5 V, the pH at the bottom of the pores becomes basic and the oxide layer is dissolved. This method reduces the risk of breaking the PAA membrane when it is removed from its growth foil. On the other hand, the authors reported a problem with corrosive pits on aluminum surface, potentially leading to the destruction of the PAA membrane. The method, as presented, is only relevant for membranes fabricated at 40 V.

Furneaux et al.[13] also used the decreasing voltage technique to etch PAA membranes anodized in H_3PO_4 at 160 V. In brief, the authors decreased the voltage by steps of 0.3 V until they reached 0.1 V. They mentioned that the current decreased significantly at each voltage drop and increased after. However, the authors did not provide any detail about the time needed to perform the entire process.

Choi et al.[14] etched PAA membranes anodized in H_3PO_4 at 195 V. They decreased the voltage by 2 V every 180 s until they reached 80 V. The anodization becoming really slow at low voltages in H_3PO_4 (low current), they completed the anodization in a 0.3 M oxalic acid solution. Using this new solution, they decreased the voltage by 2 V every 30 s for an overall process time of $\sim$ 6 hours.

As opposed to the literature above, this paper presents an etching method that can be applied to PAA membranes processed at various anodization voltages and in various solutions. Such a generic method will avoid the recourse to particular empirical recipes for each case. First of all, we develop a quantitative model to calculate the various voltages and durations involved in the process of a complete etching of the membrane, while minimizing the etching time and avoiding as much as possible pore widening. Using values calculated by the model, we gradually decrease the anodization voltage by steps, until the oxide barrier becomes completely filled with small pores, allowing us to preferentially etch the barrier and not the membrane walls in phosphoric acid. In order to avoid the use of another solution at low anodization voltages, which would allow accelerating the growth, we decided to increase the temperature instead. In this paper, we use PAA membranes made at 370 V[15] to confirm our theory. At this voltage, the pores (at a micrometer scale) are significantly larger than that of the membranes fabricated at lower voltages presented in the literature above. The resulting images with scanning electron microscopy (SEM) allow us to clearly see the network of small pores created in the oxide barrier and the preferential etching due to this network.

Quantitative Model of Barrier Etching

PAA membranes exhibit a hexagonal pore structure, which can be described using three geometrical parameters, namely the pore interval, D, the thickness of the membrane, h, and the pore diameter,

[z]E-mail: jonathan-2.bellemare@polymtl.ca

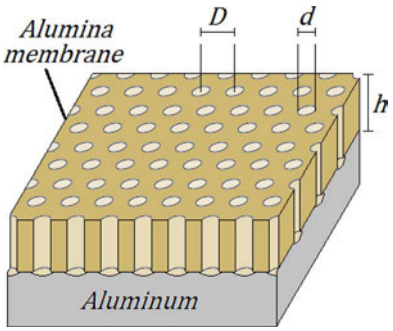

Figure 1. Schematic representation of a PAA membrane grown on an aluminum foil.

d, as shown in Fig. 1. Control over these parameters can be achieved during the fabrication of the membranes. For instance, it has been shown that pore intervals are directly proportional to the anodization voltage of the PAA membranes.[16–18] On average, the pore interval increases by 2.5 nm/V, and can be expressed as

$$D = kV, \quad [1]$$

where V is the voltage and k is a constant that may slightly differ depending on the anodization solution and its type (mild or hard).[19] Also, the membrane thickness is related to the total charge involved in the process. Time integration of the anodizing current allows calculating the total anodizing charge, Q. Reference 16 proposes a relationship between the thickness of the membrane and the anodizing current described by Eq. 2, i.e.

$$h = \frac{M}{6e\rho N_A} \frac{\int_0^T I(t)dt}{A}, \quad [2]$$

where M is the molar mass of alumina, e is the elemental charge, ρ is the density of alumina, N_A is Avogadro's number, T is the anodization time, $I(t)$ is the current as a function of time, and A is the anodized surface of the aluminum sheet.

Using values for alumina (Al_2O_3) in (2), i.e. $M = 101.96$ g/mol and $\rho = 3.97$ g/cm^3, and using the fact that the anodizing charge Q is the time integral of the anodizing current, one can rewrite Eq. 2 as

$$h = K\frac{Q}{A}, \quad [3]$$

where the membrane thickness h (in μm) is proportional to the anodizing charge Q (in mC) and inversely proportional to the anodized surface A (in cm^2), and where $K = 4.44 \times 10^{-4}$ μm $\cdot$ cm^2/mC.

The pore diameter value was obtained empirically in Ref. 20. Its value is approximately one-third that of the average inter-pore distance. It is possible to further adjust the pore diameter by post-etching of the PAA membranes in phosphoric acid.

Assuming a hexagonal structure, the surface density σ of pores can be related to the pore interval by

$$\sigma = \frac{2}{\sqrt{3}D^2}. \quad [4]$$

Substituting Eq. 1 in Eq. 4, we can see that the surface density of pores is inversely proportional to the square of the anodization voltage, i.e.

$$\sigma = \frac{2}{\sqrt{3}k^2V^2}. \quad [5]$$

This relationship will be used below to model the barrier etching process.

Let us now consider our main problem, that is, the etching of the oxide barrier at the interface between the membrane and the aluminum, i.e. at the bottom of the pores. It can be shown that the thickness of this oxide barrier, h_b, is also proportional to the anodizing voltage,[16] increasing in average by 1.1 nm/V, leading to

$$h_b = k_0 V. \quad [6]$$

Any attempts to etch this barrier in phosphoric acid will also etch the pore walls of the membrane. The oxide thickness between two pores is given by the difference between D and d, which is approximately 0.67 kV assuming a minimum value of $d = 0.33$ D. As the oxide between the two pores is consumed from both sides, we only need to etch ~ 0.34 kV to completely dissolve the pore walls. The value of 0.34 k is 0.85 nm/V, which is smaller than the value of k_0 in Eq. 6. This implies that the pore walls will be completely etched before we pierce the oxide barrier, assuming the same etching rate for both the barrier and the pore walls.

In order to preferentially etch the oxide barrier at the bottom of the pores, we can create a network of small pores in the oxide barrier: this allows increasing the dissolution rate of the barrier as compared to that of the pore walls. For this, we reduce the voltage from 370 V to 110 V by steps of $\Delta V_d = 15$ V. For each decrement of 15 V, we must use the right amount of anodizing charge: not enough charge prevent small pores to grow fast enough, whereas an excessive anodizing charge leads to the formation of a new membrane under the oxide barrier of the original PAA membrane. Therefore, we aim to only anodize a thickness $h_b = k_0 \Delta V_d$ as inferred from Eq. 6. The anodizing decrement charge, Q_d, corresponding to this thickness, can be deduced from Eq. 3. Isolating the anodizing decrement charge leads to

$$Q_d = \frac{k_0 A}{K} \Delta V_d, \quad [7]$$

where Q_d is in coulomb, A is in cm^2 and ΔV_d is in Volt. For example, a decrement of 15 V and an area of 18 cm^2 correspond to an anodizing decrement charge $Q_d = 0.67$ C. Eq. 7 assumes that all the charge takes part to the anodization process.

Calculating the ratio of the surface density of pores at 370 V and 110 V with Eq. 5, we find that there are 11.3 small pores for each pore, assuming that the pore growth in the oxide barrier is the same as that of a flat aluminum surface:

$$\frac{\sigma_{110\,V}}{\sigma_{370\,V}} = \frac{\Delta V_{370\,V}^2}{\Delta V_{110\,V}^2} = \frac{370^2}{110^2} = 11.3. \quad [8]$$

The overall process leads to the formation of a network of small pores on the oxide barrier at the bottom of the larger pores, with a pore interval of $D_{110\,V} \approx 300$ nm and an oxide barrier thickness of $h_{b110\,V} \approx 120$nm (Fig. 2) compared to $D_{370\,V} \approx 1000$ nm and $h_{b370\,V} \approx 400$ nm for the original template.

Once the network of small pores is formed, one must calculate the etching time required to completely etch the oxide barrier. This is achieved by calculating the thickness of alumina to be etched and dividing it by the etching rate. In Fig. 2a, we see that the farthest point of oxide to be etched is located at the center of the triangle of side $D_{110\,V}$. This distance is $h'_g = D_{110\,V}/(2\cos(\pi/6))$. Considering that this point has a depth of $h_{b110\,V}$, as shown in Fig. 2b, we can estimate

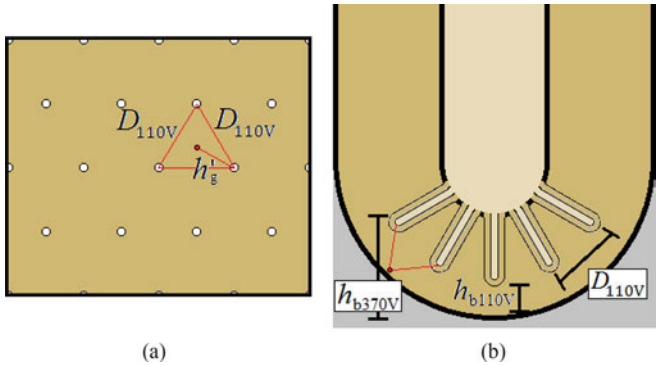

Figure 2. Schematic representation of a small pore network formed at the bottom of a PAA membrane (a) Small pore network separated by a pore interval $D_{110\,V}$ (b) Cross-section view of a pore in which a small pore network is formed.

the maximum thickness to be etched using

$$h_g = \sqrt{\left(\frac{D_{110\,V}}{2\cos\left(\frac{\pi}{6}\right)}\right)^2 + h_{b110\,V}^2}. \quad [9]$$

With values $D_{110\,V} = 300\,\text{nm}$ and $h_{b110\,V} = 120\,\text{nm}$, we find $h_g = 211\,\text{nm}$.

Using a solution of phosphoric acid 0.8 M heated at 50°C, for which the etching rate was previously determined to be 4.1 nm/min., we calculate for a thickness of 215 nm a total etching time of 53 minutes.

Experimental

We have fabricated PAA membranes using a voltage of 370 V in an electrolyte of citric acid 2% wt maintained at 20°C.[15,17] The experimental setup used a voltage source 450 V / 2 A and a 1 L solution of citric acid in an isothermal bath maintained at constant temperature, regulated within ±0.1°C. We used aluminum foils, 120 μm thick, 99.99% purity, from Hitachi AIC Inc. Haga Works. The surface of the PAA membrane was 18 cm^2 and its thickness was ∼25 μm.

The formation of the small pores at the bottom of the larger ones was carried in the same electrolyte of citric acid 2 wt%. Initially, the PAA membranes were set to 355 V, i.e. 15 V lower than their anodizing voltage, and the electrolyte bath temperature was maintained at 20°C, as can be seen in Figs. 3 and 4. The initial anodizing current could be as high as ∼4 mA. This voltage has been maintained until an anodizing charge of $Q_d = 0.67\,\text{C}$ had passed through the anodizing cell, as calculated in the previous section.

Then, during the following voltage steps, the current always showed the same pattern: a significant decrease of the current, followed by an increase at a rate of 0.5 mA/min to 2 mA/min, depending of temperature and voltage, as can be seen in Fig. 3. To accelerate the process, we increased the bath temperature at a rate of ∼80°C/h, until it reached 80°C. This temperature rise allowed us maintaining an efficient anodization as we gradually reduced the voltage by steps of 15 V, until we reached a voltage of 110 V. We made sure to let a total anodizing charge $Q_d = 0.67\,\text{C}$ pass through the cell at each step. In this particular case, at the end of the anodization process, a total charge of ∼10 C must have flowed through the anodization cell.

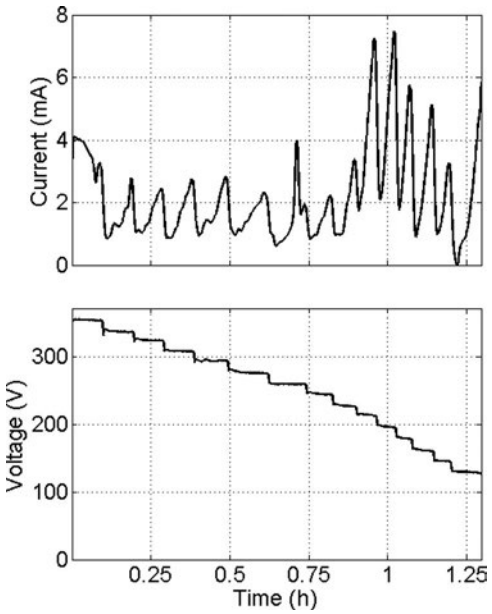

Figure 3. Current and voltage recorded during the formation of the network of small pores.

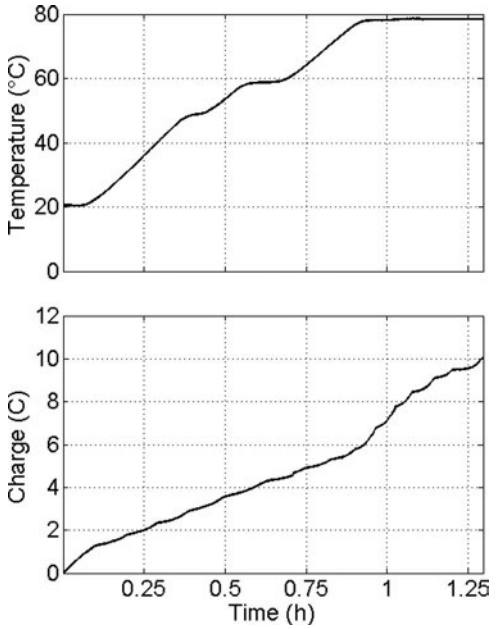

Figure 4. Temperature and charge transfer during the formation of the network of small pores. The bath temperature was initially set to 20°C, and increased by ∼80°C/h, until reaching 80°C.

Once the small pores are formed in the oxide barrier, the etching is straightforward. We prepared a 0.8 M solution of phosphoric acid heated at 50°C with an isothermal bath. Considering that the etching rate of alumina in this solution is 4.1 nm/min, we dipped the PAA membrane into the phosphoric acid solution for 53 minutes, as calculated in the previous section.

The characterization of the PAA membrane has been achieved as follows. We first detached the membrane from the aluminum surface, using a solution of perchloric acid 70% ACS reagent from Sigma-Aldrich. Again, the aluminum sheet supporting the PAA membrane constituted the anode, and a sheet of non-electropolished aluminum was used as the cathode. To detach the PAA membrane, we briefly applied a higher voltage than the last anodizing voltage of 110 V, for example 150 V. Note that this involved a high current, requiring the use of a source capable of supplying about 1 A. After a few seconds, the membrane detached itself from the aluminum substrate. The membrane was then examined using a scanning electron microscope (SEM) S-4700. Since the membrane was completely detached (free standing), it was possible to observe both its top and bottom surfaces. In order to look at the cross-section of the pores, however, we fractured the membrane in two pieces.

Results and Discussion

From the quantitative model presented above, we derived a particular recipe for a PAA membrane made at 370 V, i.e. according to Eq. 7, we have to let a total charge of ∼0.67 C flow for each 15 V step in order to create a network of small pores in the oxide barrier. This recipe was implemented to confirm that the model indeed leads to a complete and a preferential etching of the oxide barrier rather than etching of the pore walls. The results presented below confirm that it is indeed the case.

Fig. 5a shows the bottom surface of the membrane anodized at 370 V, prior to etching the barrier. The obstructed end of half of the pores, on the right-hand side of the figure, looks like broccoli or cauliflower, due to the presence of the small pores and a slight over-anodization. The other half, on the left-hand side of the figure, does not show over-anodization confirming that we are at the limit between under and over-anodization. To show that the barrier etching was successful, we observed the bottom surface of the PAA membrane

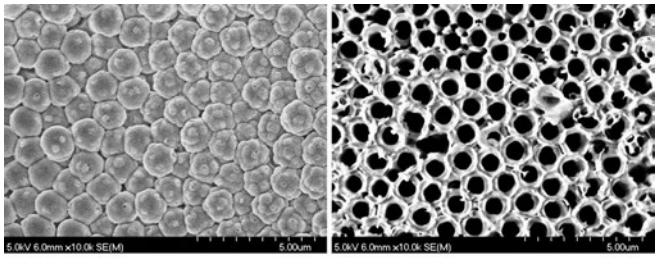

Figure 5. SEM images taken from the bottom surface of a PAA membrane formed at 370 V, in which we performed the etching of the oxide barrier (a) Membrane anodized at 370 V before the etching of the oxide barrier (b) Membrane anodized at 370 V after the etching of the oxide barrier.

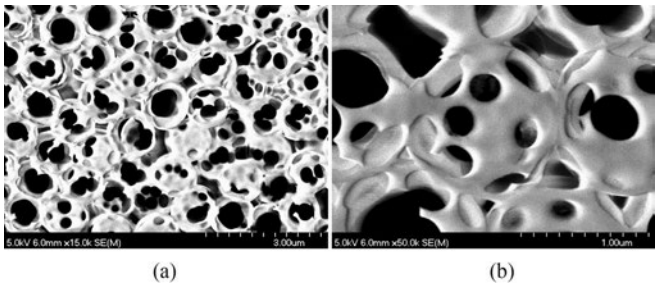

Figure 6. SEM images taken from the bottom surface of a PAA membrane formed at 370 V, in which we observe partial etching of the oxide barrier (a) 15 000X (b) 50 000X.

after etching, as shown in Fig. 5b. The presence of perforated domes on top of some of the pores, shown in greater details in Figs. 6a and 6b, is due to the residual part of the oxide barrier that was not fully etched, and confirms that we are indeed observing the bottom surface of the membrane.

Finally, to confirm the preferential etching of the oxide barrier, we stopped the phosphoric acid etching, before the 53 minutes calculated for a 215 nm thickness to etch at a rate of 4.1 nm/min. This is illustrated in Fig. 7, where we can observe the cross-section of the PAA membrane etched for less time than required for complete etching of the oxide barrier. We clearly see the preferential etching of the oxide barrier at the bottom surface of the pore walls, since the wall thickness is roughly 400 nm, whereas the residual thickness of the barrier is approximately 200 nm. We also observe a large number of small pores at the bottom of the main pore, as expected from the voltage decrease from 370 V to 110 V, which created the small pores. The thickness of the oxide barrier remained relatively unchanged, and there is no evidence of over-anodization resulting from an excessive anodizing charge. This emphasizes the importance of calculating the anodizing charge for every 15 V decrement.

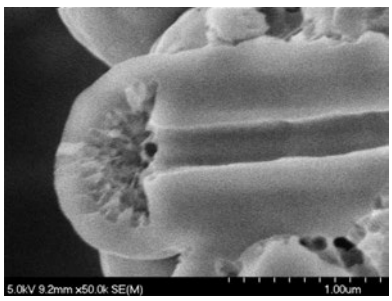

Figure 7. SEM image taken from the side of a pore where we can see the preferential etching of the barrier at the bottom of the pore and the formation of the small pores.

The minimum anodization voltage of the original template for which our barrier etching method would still be applicable remains unknown to this point. However, we are confident that our methodology can be extended to PAA obtained at lower voltages, down to 40 V, since Nielsch et al.[11] and Zhao et al.[12] created a network of small pores in PAA membranes anodized at 40 V.

Conclusions

In this paper, we developed a systematic procedure, guided by a simple quantitative model, to etch the oxide barrier at the bottom of PAA membranes. The procedure is based on the gradual decrease of the anodization voltage, i.e. from 370 V to 110 V by steps of 15 V for the example presented in this paper. Doing so leads to the formation of a network of small pores in the oxide barrier at the bottom of each pore of a PAA membrane, creating favorable conditions for etching completely the oxide barrier without over-etching the remaining of the membrane, in particular the pore walls. Further, our quantitative model could be adapted to calculate the proper etching conditions of oxide barrier of PAA membrane processed at other voltages. The complete etching of the oxide barrier was observed using SEM images. This work should enable a better control over the uniformity and geometrical parameters of PAA membranes, which are used as templates to grow nanowires or filters.

References

1. B. Kalska-Szostko, U. Wykowska, K. Piekut, and E. Zambrzycka, *Colloids and Surfaces A: Physicochemical and Engineering Aspects*, **416**, 66 (2013).
2. X. Meng, M. N. Banis, D. Geng, X. Li, Y. Zhang, R. Li, H. Abou-Rachid, and X. Sun, *Applied Surface Science*, **266**, 132 (2013).
3. M. Norek, G. Łuka, M. Godlewski, T. Płociński, M. Michalska-Domańska, and W. Stępniowski, *Applied Physics A*, **111**(1), 265 (2013).
4. J. Li, L. Zhang, J. Zhu, Y. Liu, W. Hao, and B. Li, *Materials Letters*, **87**, 101 (2012).
5. W. Liu, X. Wang, R. Xu, X. Wang, K. Cheng, H. Ma, F. Yang, and J. Li, *Materials Science in Semiconductor Processing*, **16**(1), 160 (2013).
6. A. de la Escosura-Muñiz, W. Chunglok, W. Surareungchai, and A. Merkoçi, *Biosensors and Bioelectronics*, **40**(1), 24 (2013).
7. Whatman, Anopore inorganic membranes (Anodisc), http://www.whatman.com/PRODAnoporeInorganicMembranes.aspx, (2013).
8. P. H. Lu, K. Wang, Z. Lu, A. J. Lennon, and S. R. Wenham, *IEEE Journal of Photovoltaics*, **3**(1), 143 (2013).
9. C. Y. Han, G. A. Willing, Z. Xiao, and H. H. Wang, *Langmuir*, **23**(3), 1564 (2006).
10. L.-P. Carignan, A. Yelon, D. Ménard, and C. Caloz, *IEEE Transactions on Microwave Theory and Techniques*, **59**(10), 2568 (2011).
11. K. Nielsch, F. Müller, A. P. Li, and U. Gösele, *Advanced Materials*, **12**(8), 582 (2000).
12. X. Zhao, S.-K. Seo, U.-J. Lee, and K.-H. Lee, *Journal of The Electrochemical Society*, **154**(10), C553 (2007).
13. R. C. Furneaux, W. R. Rigby, and A. P. Davidson, *Nature*, **337**(6203), 147, (1989).
14. J. Choi, G. Sauer, K. Nielsch, R. B. Wehrspohn, and U. Gösele, *Chemistry of Materials*, **15**(3), 776 (2003).
15. J. Bellemare, F. Sirois, and D. Ménard, *Journal of The Electrochemical Society*, **161**(5), E75 (2014).
16. G. D. Sulka, *Nanostructured Materials in Electrochemistry*, pp.1, Wiley, 2008.
17. S. Z. Chu, K. Wada, S. Inoue, M. Isogai, Y. Katsuta, and A. Yasumori, *Journal of The Electrochemical Society*, **153**(9), B384 (2006).
18. A. P. Li, F. Müller, A. Birner, K. Nielsch, and U. Gösele, *Journal of Applied Physics*, **84**(11), 6023 (1998).
19. L. Bruschi, G. Mistura, S.-J. Park, and W. Lee, *Adsorption*, **20**(7), 889 (2014).
20. K. Nielsch, J. Choi, K. Schwirn, R. B. Wehrspohn, and U. Gösele, *Nano Letters*, **2**(7), 677 (2002).